Taxifolin protects rat against myocardial ischemia/reperfusion injury by modulating the mitochondrial apoptosis pathway

Zhenqiu Tang[1,†], Chunjuan Yang[2,3,†], Baoyan Zuo[4], Yanan Zhang[1], Gaosong Wu[1], Yudi Wang[1], Zhibin Wang[1], *

[1] Key Laboratory of Chinese Materia Medica, Heilongjiang University of Chinese Medicine, Harbin, Heilongjiang, China

[2] College of Pharmacy, Harbin Medical University, Harbin, Heilongjiang, China

[3] Beijing Shunyue Technology Co., Ltd., Beijing, China

[4] School of Pharmacy, Shenyang Pharmaceutical University, Shenyang, Liaoning, China

[†] These authors contribute equally to this paper.

Corresponding Author:

Zhibin Wang

No. 24 Heping road, Harbin, Heilongjiang, 150040, China

Email address: wzbmailbox@hljucm.net

ABSTRACT

Background: Taxifolin (TAX), is an active flavonoid, that plays an underlying protective role on the cardiovascular system. This study aimed to evaluate its effect and potential mechanisms on myocardial ischemia/reperfusion (I/R) injury.

Methods: Healthy rat heart was subjected to I/R using the Langendorff apparatus. Hemodynamic parameters, including heart rate (HR), left ventricular developed pressure (LVDP), maximum/minimum rate of the left ventricular pressure rise ($+dp/dt_{max}$ and $-dp/dt_{min}$) and rate pressure product (RPP) were recorded during the perfusion. Histopathological examination of left ventricular was measured by hematoxylin-eosin (HE) staining. Creatine

29 kinase-MB (CK-MB) and lactate dehydrogenase (LDH) activities in the effluent perfusion, and
30 the levels of malondialdehyde (MDA), superoxide dismutase (SOD) and glutathione peroxidase
31 (GSH-PX)   in the tissue were assayed. Apoptosis related proteins, such as B-cell lymphoma-2
32 (Bcl-2), Bcl2-associated X (Bax) and cytochrome c (Cyt-c) were also assayed by ELISA.
33 Western blot was employed to determine apoptosis-executive proteins, including caspase 3 and
34 9. TUNEL assay was performed to evaluate the effect TAX on myocardial apoptosis.

35 **Results:** TAX significantly improved the ventricular functional recovery, as evident by the
36 increase in LVDP, +dp/dt$_{max}$, -dp/dt$_{min}$ and RPP, The levels of SOD, GSH-PX were also
37 increased, but those of LDH, CK-MB, and MDA were decreased. Furthermore, TAX up-
38 regulated the Bcl-2 protein level but down-regulated the levels of Bax, Cyt-c, caspase 3 and 9
39 protein, thereby inhibits the myocardial apoptosis.

40 **Discussion:** TAX treatment remarkably improved the cardiac function, regulated oxidative stress
41 and attenuated apoptosis. Hence, TAX has a cardioprotective effect against I/R injury by
42 modulating mitochondrial apoptosis pathway.

43

INTRODUCTION

45   Ischemic heart disease is a threat to human health. Extracorporeal circulation and coronary
46 bypass surgery are usually employed to improve myocardial ischaemia after myocardial
47 infarction occurs. The timely restoration of blood flow to the ischemic myocardium (reperfusion)
48 became the standard treatment for these patients. However, reperfusion may cause additional
49 heart damage. This condition is referred to as cardiac ischaemia/reperfusion (I/R) injury
50 (*Braunwald et al., 2012*). The reperfusion of ischaemic tissues is often associated with
51 microvascular dysfunction. The mechanisms may involve the release of oxygen radicals and
52 inflammatory mediators (*Carden et al., 2000*). Nowadays, tissue injury induced by I/R is a major
53 factor, which often cause death. During myocardial I/R injury, cardiomyocytes undergo death at
54 an increased frequency, mainly including necrosis and apoptosis (*Gottlieb et al., 1994*).
55 Apoptosis involves programmed cell death, which is the vital pathological process in acute
56 reperfusion injury (*Konstantinidis et al., 2012*). When the amount of cardiomyocyte decreases,
57 the heart may undergo ventricular remodelling, compensatory cardiac hypertrophy and
58 eventually lead to heart failure (*Pangonyte et al., 2008; Du et al., 2010*). Therefore, exploring the
59 detailed mechanisms that trigger cardiomyocyte death and the means to prevent it during I/R
60 injury is still a public issue.
61   In I/R injury, morphological changes in myocardial tissue can be observed, including
62 microvascular damage and myocardial cell edema. The symptoms of I/R include myocardial
63 enzyme release, arrhythmias and weak systolic function (*Naito et al., 2000*). Generally, this
64 reperfusion damage is caused by increased free radical activity. When circulating blood
65 decreases, the level of oxygen supply cannot sustain the oxygen demand by cardiomyocytes, and

66 the aerobic metabolism turns into anaerobic metabolism (*Giordano et al., 2005*). Anaerobic
67 metabolism leads to the production of lactic acid which results in disturbances in ionic
68 homeostasis. A timely reperfusion is crucial for the recovery of an ischemic myocardium, but by
69 the sudden re-appearance of circulating blood to the dying myocardium, oxygen species (ROS)
70 will be produced as a response to hyperoxia which can worsen the functional situation of the
71 organization (*Akhlaghi et al., 2009*).

72   Flavonoid is the most prevalent class of naturally occurring compound and is ubiquitous in
73 woody and herb plants. It exerts multiple biochemical properties and wide pharmacological
74 effects (*Moon et al., 2006*). Epidemiological studies have shown that flavonoid is associated with
75 a reduced risk of cardiovascular diseases (*Raj Narayana et al., 2001*; *Bjorklund et al., 2017*).
76 Fisetin, a plant-derived bioflavonoid, significantly attenuated I/R-induced tissue injury, blunted
77 the oxidative stress, and restored mitochondrial structure and function (*Shanmugam et al., 2018*).
78 Quercetin has been demonstrated to improve post ischemic recovery of the isolated heart of rats
79 after global ischemia (*Barteková et al., 2010*). TAX exerts anti-inflammatory effects and
80 prevents oxidative stress-induced injury in human endothelial cells (*Guo et al., 2015*) and rat
81 peritoneal macrophages (*Arutyunyan et al., 2016*). It also possesses free radical scavenging,
82 antioxidant and anti-inflammatory effects (*Sun et al., 2014*; *Xie et al., 2017*). TAX is structurally
83 similar to quercetin. Hence, we suspect that it also has a beneficial effect on the cardiovascular
84 system. Recent studies demonstrated that TAX could inhibit cardiac hypertrophy and attenuate
85 ventricular fibrosis after pressure overload. These beneficial effects were at least mediated by
86 suppressing oxidative stress and the excess production of ROS. (*Guo et al., 2015; Sun et al.,*
87 *2014*). However, the potential of TAX for I/R protection remains unclear. TAX is a potential
88 candidate for the prevention or treatment for I/R injury. However, the influence of TAX on the
89 injury of I/R in isolated rat hearts has not been reported. In this study, we aimed to evaluate the
90 cardioprotective effects of TAX and investigated the mechanisms underlying these effects in
91 isolated hearts of rats.

92   Myocardial ischemic events are unpredictable. The clinical application of pre-conditioning
93 drugs is limited. Therefore, researchers turned to a new endogenous protective strategy, which is
94 post-conditioning. In 2006, the protective effect of post-conditioning in ischemic reperfusion on
95 cerebral ischemia was first reported (*Zhao et al., 2006*). Subsequent studies have validated the
96 protective effect of post-conditioning in various global ischemia models *ex vivo* and ischemia
97 and hypoxia models *in vitro*. Flavonoids reduce the injury of myocardial ischemia on perfusion
98 in a post-conditioning way (*Wang et al., 2017; Xuan et al., 2016*). Therefore, we adopted the
99 post-conditioning method in this study.

100

MATERIALS & METHODS

Experimental animals and treatment

103   Male SD rats (280-300 g each) were obtained from the Laboratory Animal Center of

104 Heilongjiang Medicine University Medical (License Number: SCXK (hei) 2013-004). The rats
105 were housed under standard conditions with natural light (12 hr) and dark (12 hr) at 22 ± 2 °C.
106 Rats were fed with common laboratory chow and allowed to drink tap water ad libitum during
107 the experimental period. The investigation conformed to Guide for the Care and Use of
108 Laboratory Animals (revised, 1996, http://dels.nas.edu/resources/static-assets/ilar/miscellaneous
109 /GUIDE1996.pdf). All animal experiments were approved by the College of Pharmacy of
110 Heilongjiang University of Chinese Medicine, Animal Ethics Committee (Approval number:
111 SYXK (hei)-2013-012).
112

Reagents and antibodies

114 TAX (purity ≥ 98%) was purchased from Sigma-Aldrich (St. Louis, MO, USA). Creatine
115 kinase-MB (CK-MB), lactate dehydrogenase (LDH), malondialdehyde (MDA) glutathione
116 peroxidase (GSH-PX) and superoxide dismutase (SOD) assay kit were obtained from Nanjing
117 Jiancheng Bioengineering Institute (Jiangsu, China). The enzyme-linked immunnosorbent assay
118 kit about mitochondrial apoptosis [B-cell lymphoma-2 (Bcl-2), Bcl2-associated X (Bax) and
119 cytochrome c (Cyt-c)] was obtained from Cloud-Clone Corp (Houston, TX, USA). Monoclonal
120 primary antibodies anti-β-actin, anti-active caspase 3 and 9 were purchased from Abcam (MA,
121 USA). Fluorescent-labeled goat anti-rabbit IgG secondary antibody was obtained from LI-COR
122 Biosciences (Lincoln, Nebraska, USA).
123

Experimental protocol

125 TAX was dissolved in ethanol (15.21, 45.63 mg/ml) and then transferred into Krebs–Henseleit
126 (K-H) solution. Ethanol solution (0.1 mL) was added into 1 L K-H solution. The final
127 concentration was 5 or 15 μM. Rats were randomly divided into four groups (n=8): Normal
128 control group (Control); Myocardial I/R control group (I/R); I/R + TAX 5 μM treatment group
129 (TAX 5 μM); I/R + TAX 15 μM treatment group (TAX 15 μM). The experimental protocol is
130 shown in Fig. 1. Control group: The hearts were subjected a continuous perfusion of K–H
131 solution for 120 min. I/R group: The hearts were perfused for 30 min to stabilization.
132 Subsequently, global ischemia was performed at 37 °C for 30 min, followed by reperfusion with
133 K–H solution for 60 min. TAX 5 μM group: The hearts were perfused for 30 min to stabilization.
134 Subsequently, global ischemia was performed for 30 min at 37 °C, followed by reperfusion with
135 5 μM of TAX-saturated K–H solution for 60 min. TAX 15 μM group: The hearts were perfused
136 for 30 min to stabilization. Subsequently, global ischemia was performed for 30 min, followed
137 by reperfusion perfused with 15 μM of TAX-saturated K–H solution for 60 min.
138

Langendorff preparation

140 After anesthetization via intraperitoneal injection (chloral hydrate solution, 300 mg/kg), rat
141 hearts were quickly removed and subsequently perfused in the Langendorff apparatus. The
142 perfusion was performed for 30 min in a modified K-H buffer gassed with 95 % O_2 and 5 % CO_2
143 at a constant flow velocity and constant temperature (37 °C). The composition of K-H buffer as

144   the following (mM): NaCl 118, MgSO$_4$ 1.2, KCl 3.2, NaHCO$_3$ 25, KH$_2$PO$_4$ 1.18, CaCl$_2$ 2.5 and
145   glucose 5.5. After equilibration, 30 min global ischemia was induced followed by 60 min of
146   reperfusion. Control group utilized the same protocol, but no ischemic induction was used.
147   Water-filled balloon that is inserted into the left ventricular cavity was used to monitor
148   hemodynamic parameters. The left ventricular end-diastolic pressure (LVEDP) was maintained
149   at 5-10 mmHg by adjusting the size and position of the balloon. The whole procedure was
150   completed within 2 min. The inclusion criteria of experimental samples were a heart rate (HR) of
151   > 250 beats/min and a left ventricular developed pressure (LVDP) of > 75 mmHg in equilibrium
152   period. In the experiment, we prepared 12 rats in each group with an average of three or four
153   failures. Finally, only eight rats from each group were used in the subsequent experiment. The
154   hemodynamic parameters were recorded during perfusion, including heart rate (HR), LVDP, the
155   maximum/minimum rate of left ventricular pressure rise (+dp/dt$_{max}$ and -dp/dt$_{min}$), which are
156   important indices to evaluate the left ventricular systolic and diastolic function. Rate pressure
157   product (RPP) =HR × LVDP. After 60 minutes of reperfusion, heart tissue was taken from
158   Langendorff apparatus. The left ventricles of three hearts were cut from each group and then
159   fixed in 10 % neutral formalin. The other tissues were immediately placed in the freezer at −80
160   °C.
161

Histopathological evaluation of left ventricle sections

163   For histopathological examination, the cut left ventricle of heart tissues were fixed in 10 %
164   neutral formalin at room temperature. After 2 hours, the tissue piece was embedded in paraffin.
165   Next, the piece was cut into 3 μm thick tissue sections, after which it was subjected to
166   hematoxylin-eosin (H&E) staining. At least three samples from each group were evaluated. The
167   tissue sections were visualized under light microscope (Olympus BX60, Tokyo, Japan).
168

Estimation of cardiac damage

170   In present study, heart tissue injury was assessed by determining the concentration of LDH
171   and CK-MB in the perfusate. The LDH and CK-MB content in the perfusate were measured
172   using the assay kit following the manufacturer's instructions. Samples of the perfusate were
173   collected from the isolated heart at 25, 63, 90 and 120 min of perfusion.
174

Measurements of anti-oxidant indices

176   The hearts tissue was cut into small pieces of tissue and then was ground with lysate buffer by
177   using a glass homogenizer. Supernatant of tissue homogenate was frozen for each tissue analysis.
178   MDA, SOD and GSH-PX activity were assessed using commercial ELISA kits following the
179   manufacturer's instructions. All enzyme activities were normalized to the total protein
180   concentrations, which were determined using a bicinchoninic acid (BCA) protein assay kit
181   (Beyotime, Shanghai, China).
182

Estimation of Cyt-c, Bcl-2 and Bax levels

184   Following the instructions of nuclear and cytoplasmic protein extraction kit (Beyotime,
185 Shanghai, China), heart tissue samples were weighed, minced into small pieces and
186 homogenized using a glass homogenizer on ice (w: v = 1:30, 1 mL lysis buffer was added in 30
187 mg tissue sample). The homogenates were centrifuged at 1500× g for 5 min at 4 °C and the
188 cytoplasmic protein was obtained from the supernatant. The Cyt-c, Bcl-2 and Bax protein levels
189 were measured according to the manufacturer's instructions of commercial kits through an
190 ELISA-type method (Cloud Clone Corp, Houston, USA).
191

Western blotting analysis

193   Myocardial tissue samples were lysed with RIPA buffer containing protease inhibitors for 15
194 min on ice. The total lysates were clarified by centrifugation, and supernatants were collected.
195 Protein samples (20-25 mg per lane) were loaded on the gels and then separated by 10 % sodium
196 dodecyl sulfate-polyacrylamide gel electrophoresis (SDS-PAGE) under reducing conditions and
197 transferred onto the nitrocellulose membrane (Roche, Mannheim, Germany). The membrane was
198 washed with PBS with 0.1% Tween-20 (PBST) and blocked with 5% skim milk in shaking table
199 for 2 h at room temperature. Then the membrane was washed with PBST and incubated with
200 antigen-specific rabbit IgG antibodies (anti-caspase 3 and 9, anti-β-actin; Abcam) diluted to
201 1:1000 in PBST. Next, the membrane was washed with PBST and incubated with fluorescent-
202 labeled goat anti-rabbit secondary antibodies (LI-COR, Lincoln, Nebraska, USA) diluted to
203 1:2500 in PBST for 2 h at 4 °C. The target protein bands were scanned using the blot imaging
204 system GelLogic 212 PRO (Carestream, Rochester, NY, USA) after washing with PBST. The
205 obtained images were quantified as the final results by image J 1.4.3 (www.imagej.nih.gov/ij).
206 The results were expressed as the fold induction, which were than compared with the normal
207 control.
208

TUNEL assay

210   Heart sections of 3 μm thickness were obtained using a microtome. The sections were
211 deparaffinized in xylene and rehydrated in concentration gradient of ethanol (100%, 95%, 75%).
212 Following this, sections were then incubated with proteinase K and with 30% H_2O_2 to enhance
213 tissue permeability and diminish any endogenous peroxidase activity respectively. Apoptosis
214 was determined using a terminal deoxynucleotidyl transferase-mediated dUTP-X nick end
215 labeling (TUNEL) assay kit (Roche, Basel, Switzerland) according to the manufacturer's
216 protocol. The sections were incubated with complete labeling reaction buffer for 60 min and
217 antibody solution for 30 min. Chromogenic reaction was visualized using 3,3-diaminobenzidine
218 (DAB). Sections were visualized under light microscope (Olympus BX60, Tokyo, Japan).
219

Statistical Analysis

221   SPSS16.0 for Windows (SPSS Inc., Chicago, USA) was used for statistical analysis. All data
222 were expressed as mean ± standard deviation (SD). For comparisons between groups, the one-

223   way ANOVA or student T-test was used where appropriate. Statistical differences were
224   considered significant at P < 0.05. # P < 0.05 and ## P < 0.01 vs. control group. * P < 0.01 and
225   ** P < 0.001 vs. I/R group.

226

227   RESULTS

228   Effects of TAX on Cardiac Parameters of Isolated Hearts

229   We examined whether TAX could protect the hearts of rat against *ex vivo* I/R injury. Results
230   showed no obvious alteration in the average HR of isolated heart during reperfusion with or
231   without TAX. In addition, no significant HR change was observed between I/R and normal
232   groups during the 30 min of ischemia and 60 min of reperfusion (Fig. 2A). After reperfusion,
233   LVDP, +dp/dt$_{max}$ and -dp/dt$_{min}$ from different treatment groups decreased in varying degrees. For
234   instance, LVDP was significantly increased in TAX 15 μM group compared with I/R group at
235   the end periods of reperfusion (LVDP = 68 mmHg vs. 52 mmHg, P < 0.05, Fig. 2B). In
236   comparison with I/R group, treatment with 15 μM TAX significantly improved the RPP in rat at
237   60 min of reperfusion (RPP = 15294 mmHg × beats/min in TAX vs. 10643 mmHg × beats/min
238   in I/R, P < 0.01, Fig. 2E). Results showed that TAX treatment improved the cardiac function
239   recovery of rats during myocardial I/R injury.

240

241   TAX Down-regulated the Release of LDH and CK-MB

242   At different time points of perfusion, heart effluents were collected. The LDH level in the
243   whole perfusion process was not conspicuously altered in control group. The perfusate LDH
244   activity of I/R group was improved compared with that of control group after reperfusion and
245   was significantly increased at 60 min of reperfusion (P < 0.01). TAX highly reduced the LDH
246   levels compared with I/R group at 60 min of reperfusion (Fig. 3A). CK-MB release was similar
247   to the LDH release. The expression in the whole perfusate process was not conspicuously
248   changed in the control group. In the perfusion stabilization, no significant difference was
249   observed in the CK-MB level among the four groups. However, the levels in I/R group were
250   markedly higher after 30 min of reperfusion compared with perfusion stabilization (P < 0.05).
251   Interestingly, the CK-MB release in both TAX 5 and 15 μM group was significantly decreased at
252   end of reperfusion compared with I/R group (P < 0.05 or P < 0.01) (Fig. 3B). These results
253   indicated that TAX could protect the cardiac function against I/R injury.

254

255   Effect of TAX on Myocardial Morphology

256   Histopathological examination of myocardial tissue was assessed by H&E staining. Typical
257 micrographs of the myocardial structure are shown in Fig. 4. In control group (Fig. 4A), The
258 morphology of the myocardial tissue was normal. Cardiomyocytes are arranged closely, the
259 intercellular space is small, and edema does not exist between cells. By contrast, I/R group (Fig.
260 4B) showed degenerated muscle fibers and obvious contraction band, severe obvious cells
261 edema, many infiltrated inflammatory cells. Fig. 4C shows that the TAX 5 μM group maintained
262 the myocardium with only slightly irregularly arranged fibers and a few contraction bands. Fig.
263 4D shows that the TAX 15 μM group showed orderly cardiomyocytes but a few cell dissolution
264 and degeneration. Results showed that treatment with 15 μM TAX significantly reduced I/R
265 injury compared with I/R group.

266

Effect of TAX on I/R-induced Oxidative Stress in the Myocardium

268   To explore the cardio-protective mechanism of TAX, the effects of TAX on SOD, GSH-PX
269 and MDA activity were investigated in myocardial tissue in response to I/R injury. Fig. 5 shows
270 that TAX 15 μM group, the SOD and GSH-PX activity were increased significantly compared
271 with those of in I/R group (P < 0.01), whereas no significant difference was observed in the TAX
272 5 μM group. Conversely, these TAX treatment groups showed that MDA production was
273 significantly reduced (P < 0.01) compared with I/R group.

274

TAX Protects Myocardial Cell from I/R-induced Mitochondrial Damage

276   To evaluate if the effect of TAX is mediated through attenuation of the mitochondrial damage,
277 we determined cytochrome c (Cyt-c) in cytosol. Fig. 6A shows that I/R increased the cytosolic
278 Cyt-c levels (P < 0.01). By comparison, TAX at different doses could reduce I/R-induced
279 increase of Cyt-c levels (P < 0.01). The result suggested that TAX attenuated I/R induced Cyt-c
280 release to the cytosol. The Bcl-2 family of proteins modulates the release of Cyt-c by regulating
281 mitochondrial transmembrane potential. We also determined Bcl-2 and Bax protein levels.
282 Compared with the control group, I/R down-regulated Bcl-2 but up-regulated Bax protein
283 expression (Figs. 6B-6C). TAX increased Bcl-2 levels but decreased Bax levels compared with
284 I/R. These results indicate that TAX may protect mitochondria against apoptosis by regulating
285 the expression of the Bcl-2 family proteins.

286

TAX Attenuates Myocardial I/R-induced Apoptosis

288   To explore the potential mechanism of TAX in rats subjected to I/R-induced myocardial
289 injury, we investigated the protein expressions of active-caspase 3 and 9. Compared with control

290   group, the expression of active-caspase 3 was up-regulated in I/R group. While compared with
291   I/R group, TAX treatment group significantly reduced the level of active-caspase 3 (Fig. 7C). In
292   TAX treatment group, the expression of active-caspase 9 was down-regulated in 15 μM (P<
293   0.05), but did not change significantly in 5 μM (Fig. 7D). In addition, TUNEL assay was
294   performed to evaluate the effect TAX on myocardial apoptosis. An increased number of TUNEL
295   positive cells were observed in I/R group in comparison to control group. Furthermore, a less
296   number of TUNEL positive cell was present in the TAX treatment group (Fig. 8). Results
297   indicated that TAX inhibited apoptotic level in heart injury induced by I/R.

298

DISCUSSION

300   Growing evidence indicates a therapeutic action of TAX in cardiovascular disease. However,
301   the implications of TAX in I/R injury remain unclear. To the best of our knowledge, this study
302   was the first to evaluate the cardioprotective effects of TAX in isolated rat heart subjected to I/R
303   injury. We demonstrated that an important role of TAX in improving cardiac function, and
304   inhibiting oxidative stress and apoptosis in a model of I/R injury *in vitro*.

305   In the late 19th century, Oscar Langendorff pioneered the isolated perfused heart model. Since
306   then, the procedure has been used to probe the pathophysiology of I/R with the dawn of
307   molecular biology (*Bell et al., 2011*). Today, the Langendorff heart assay is a predominant
308   technique *in vitro*, which is used in physiological and pharmacological research. It allows the
309   examination of cardiac contractile strength and heart rate without complications of an intact
310   animal (*Herr et al., 2015*). Therefore, we determined the effect of TAX to the cardiac function
311   parameters of isolated heart in myocardial I/R injury by using the Langendorff equipment.
312   Cardiac functions mainly depend on the contraction and relaxation properties of the ventricular
313   muscle. Changes in cardiac function are strongly linked to the severity of I/R injury (*Mehdizadeh*
314   *et al., 2013*). The data from our analyses showed that I/R can cause marked myocardial
315   dysfunction, including the reduction of LVDP, $+dp/dt_{max}$ and $-dp/dt_{min}$. TAX treatment
316   significantly improved cardiac diastolic dysfunction but did not alter the average HR in isolated
317   heart.

318   LDH is a marker of cellular damage and common disease due to its mass release to plasma
319   during tissue injuries, such as heart failure. CK-MB, which is expressed extensively in cardiac
320   myocyte, was often tested in the serum as an indicator of rhabdomyolysis damage, myocardial
321   damage and acute kidney injury in clinic (*Moghadam-Kia et al., 2016*). The increase in LDH and
322   CK-MB levels in the organ perfusate after ischemia is a direct evidence of cardiac damage
323   (*Houshmand et al., 2009*). In comparison with control group, LDH and CK-MB activity were
324   significantly increased in I/R group during myocardial I/R injury. Perfusate LDH and CK-MB
325   activity in the TAX treatment groups, particularly in TAX 15 μM group, were remarkably
326   reduced compared with those in I/R group, which is consistent with the observation of changing
327   cardiac function parameters. In addition, histopathological examination was implemented to

328   assess the effect of TAX on myocardial morphology. The results of pathomorphological research
329   in the heart samples in I/R group show acute myocardial damage, and TAX causes favorable
330   morphological changes in the heart during I/R injury. These results supported the potential
331   application of TAX as a cardioprotective agent in myocardial I/R injury.

332   Under normal conditions, tissues could maintain the balance between generation and clearance
333   of ROS. However, the balance is disrupted during I/R and causes significant increase in ROS
334   (*Becker et al., 2004*). Excess ROS can oxidize lipids, proteins and DNA, which cause
335   dysfunction of these molecules, resulting in the degeneration of tissue function (*Kleikers et al.,*
336   *2012*). Minimizing the ROS production is an important strategy to prevent cardiomyocyte I/R
337   injury (*He et al., 2016*). Therefore, the activation of the anti-oxidant enzyme system is necessary
338   to reduce oxidative stress-induced tissue damage (*Matsushima et al, 2013*). The SOD and GSH-
339   PX rate are used to evaluate tissue per-oxidative injury (*Maciejczyk et al., 2017*). In addition,
340   MDA is an index to evaluate the severity of lipid peroxidation, which is produced by lipid
341   peroxidation, resulting in the destruction of structural proteins and cellular structures (*Pizzimenti*
342   *et al., 2013*). Our results showed that SOD and GSH-PX activities were conspicuously increased,
343   whereas MDA level was dramatically decreased by TAX, especially in TAX 15 μM group.
344   Therefore, TAX exhibited the cardioprotective effects by enhancing the antioxidase activity and
345   inhibiting free radical peroxidation.

346   Mitochondrial damage plays an important role in I/R-induced injury. It is the final arbitrator
347   for I/R-induced cell apoptosis (*Powers et al., 2007*). During ischemia and mainly during the
348   early period of reperfusion, excessive ROS causes myocardial Ca^{2+} overload and the opening of
349   the mitochondrial permeability transition pore (mPTP), which can reduce mitochondrial function
350   and finally result in an increase in myocardial cell apoptosis (*Garciarena et al., 2011*; *Halestrap*
351   *et al., 2015*). One of the ways of cell apoptosis is activated by the release of Cyt-c from the
352   mitochondria to the cytosol. In our study, results showed that TAX can weaken the observed
353   increase in the expression of Cyt-c in cytosol. It is very likely that the increased cytosolic content
354   of Cyt-c, which mediates apoptosis, while its expression in mitochondria was not changed
355   (*Lundberg et al., 2004*). Further investigation of the pathological changes in myocardial tissues
356   by TUNEL assays showed different degrees of apoptosis. Results indicated a positive effect of
357   TAX in the inhibition of apoptosis. Therefore, it can make an assumption that down-regulation
358   of Cyt-c result from TAX attenuated apoptotic processes.

359   As an important mitochondrial regulator during myocardial apoptosis, Bcl-2 exerts anti-
360   apoptotic effects by blocking the release of Cyt-c and reducing caspase activity. Apoptosis-
361   related proteins, caspase 3 and 9, also play crucial roles in apoptosis. The caspase apoptotic
362   pathway responds to death signals by releasing apoptosis-inducing factor from the mitochondria,
363   which were then translocated to the nucleus (*D'Amelio et al., 2012*). In this study, Bcl-2, an anti-
364   apoptotic protein and Bax, a pro-apoptotic protein were used to assess the effects of TAX on
365   cardiomyocytes apoptosis. The result demonstrated that TAX treatment increased the protein
366   expression of Bcl-2, and significantly reduced the Bax expression compared with I/R group.

367 Caspase 3 and 9 were tested to measure the apoptotic level in the isolated heart after I/R injury.
368 We found that the increased expression of the active form of caspase 3 and 9 under ischemic
369 conditions and their expression were decreased in TAX group. Consistent with these results,
370 treatment with TAX significantly decreased myocardial apoptosis by regulating the expression of
371 apoptosis-related proteins, including Bax, Bcl-2 and caspase 3 and 9. These findings suggest that
372 the inhibition of apoptosis is closely related to the underlying beneficial effect of TAX in I/R
373 injury. Cardiomyocytes death occurs during I/R injury by apoptosis, by necrosis and in
374 association with autophagy (*Whelan et al., 2010; Gatica D et al., 2015*). In this study, we studied
375 the effect of apoptosis on myocardial injury, but the effect of other pathways on myocardial
376 injury was not excluded, which requires further exploration.

377

CONCLUSIONS

379   In conclusion, TAX exerted cardioprotective effects against I/R injury by inhibiting oxidative
380 stress and cardiac myocyte apoptosis. The underlying mechanism for these phenomena may
381 involve modulation of mitochondrial apoptosis pathway. Our finding provides a novel thought
382 for therapeutic development as an adjuvant therapy to I/R injury.

383

REFERENCES

385 **Akhlaghi M, Bandy B. 2009.** Mechanisms of flavonoid protection against myocardial ischemia–
386 reperfusion injury. *Journal Molecular Cellular Cardiology* **46(3)**:309–317.
387 **Arutyunyan TV, Korystova AF, Kublik LN, Levitman MKh, Shaposhnikova VV, Korystov**
388 **YN. 2016.** Taxifolin and fucoidin abolish the irradiation-induced increase in the production of
389 reactive oxygen species in rat aorta. *Bulletin of Experimental Biology and Medicine* **160(5)**:635–
390 638.
391 **Barteková M, Carnická S, Pancza D, Ondrejcáková M, Breier A, Ravingerová T. 2010.**
392 Acute treatment with polyphenol quercetin improves postischemic recovery of isolated perfused
393 rat heart after global ischemia. *Canadian Journal of Physiology and Pharmacology* **88(4)**:465–
394 471.
395 **Becker LB. 2004.** New concepts in reactive oxygen species and cardiovascular reperfusion
396 physiology. *Cardiovascular Research* **61(3)**:461–470.
397 **Bell RM, Mocanu MM, Yellon DM. 2011.** Retrograde heart perfusion: the Langendorff
398 technique of isolated heart perfusion. *Journal of Molecular and Cellular Cardiology* **50(6)**:940–
399 950.
400 **Bjorklund G, Dadar M, Chirumbolo S, Lysiuk R. 2017.** Flavonoids as detoxifying and pro-
401 survival agents: what's new? *Food and Chemical Toxicology* **110**:240–250.
402 **Braunwald E. 2012.** The treatment of acute myocardial infarction: the past, the present, and the

403   future. *European Heart Journal of Acute Cardiovascular Care* **1(1)**:9–12.

404   **Carden DL, Granger DN. 2000.** Pathophysiology of ischaemia-reperfusion injury. *Journal of*
405   *Pathology* **190**: 255–266.

406   **Chong SJ, Low IC, Pervaiz S. 2014.** Mitochondrial ROS and involvement of Bcl-2 as a
407   mitochondrial ROS regulator. *Mitochondrion* **19**:39–48.

408   **D'Amelio M, Sheng M, Cecconi F. 2012.** Caspase-3 in the central nervous system: beyond
409   apoptosis. *Trends in Neurosciences* **35(11)**:700–709.

410   **Dianzani C, Lepore A, Gentile F, Barrera G. 2013.** Interaction of aldehydes derived from lipid
411   peroxidation and membrane proteins. *Frontiers in Physiology* **4**:242.

412   **Du Y, Plante E, Janicki JS, Brower GL. 2010.** Temporal evaluation of cardiac myocyte
413   hypertrophy and hyperplasia in male rats secondary to chronic volume overload. *American*
414   *Journal of Pathology* **177(3)**:1155–1163.

415   **Garciarena CD, Fantinelli JC, Caldiz CI, Chiappe de Cingolani G, Ennis IL, Perez NG,**
416   **Cingolani HE, Mosca SM. 2011.** Myocardial reperfusion injury: reactive oxygen species vs.
417   NHE-1 reactivation. *Cellular Physiology and Biochemistry* **27(1)**:13–22.

418   **Gatica D, Chiong M, Lavandero S, Klionsky DJ. 2015.** Molecular mechanisms of autophagy
419   in the cardiovascular system. Circulation Research **116**:456**–**467.

420   **Giordano FJ. 2005.** Oxygen, oxidative stress, hypoxia, and heart failure. *Journal Clinical*
421   *Investigation* **115(3)**:500–508.

422   **Gottlieb RA, Burleson KO, Kloner RA, Babior BM, Engler RL. 1994.** Reperfusion injury
423   induces apoptosis in rabbit cardiomyocytes. *Journal of Clinical Investigation* **94(4)**:1621–1628.

424   **Guo H, Zhang X, Cui Y, Zhou H, Xu D, Shan T, Zhang F, Guo Y, Chen Y, Wu D. 2015.**
425   Taxifolin protects against cardiac hypertrophy and fibrosis during biomechanical stress of
426   pressure overload. *Toxicology and Applied Pharmacology* **287(2)**:168–177.

427   **Halestrap AP, Richardson AP.** 2015. The mitochondrial permeability transition: a current
428   perspective on its identity and role in ischaemia/reperfusion injury. *Journal of Molecular and*
429   *Cellular Cardiology* **78**:129–141.

430   **He F, Li J, Liu Z, Chuang CC, Yang W, Zuo L. 2016.** Redox mechanism of reactive oxygen
431   species in exercise. *Frontiers in Physiology* **7**:486.

432   **Herr DJ, Aune SE, Menick DR. 2015.** Induction and Assessment of Ischemia-reperfusion
433   Injury in Langendorff-perfused Rat Hearts. *Journal of Visualized Experiments* **101**:e52908.

434   **Houshmand F, Faghihi M, Zahediasl, S. 2009.** Biphasic protective effect of oxytocin on
435   cardiac ischemia/reperfusion injury in anaesthetized rats. *Peptides* **30(12)**:2301–2308.

436   **Kleikers PW, Wingler K, Hermans JJ, Diebold I, Altenhöfer S, Radermacher KA, Janssen**
437   **B, Görlach A, Schmidt HH. 2012.** NADPH oxidases as a source of oxidative stress and
438   molecular target in ischemia/reperfusion injury. *Journal of Molecular Medicine (Berlin)*
439   **90(12)**:1391–1406.

440   **Konstantinidis K, Whelan RS, Kitsis RN. 2012.** Mechanisms of cell death in heart disease.
441   *Arteriosclerosis Thrombosis Vascular Biology* **32(7)**:1552–1562.

442 **Lundberg KC, Szweda LI. 2004.** Initiation of mitochondrialmediated apoptosis during cardiac
443 reperfusion. *Archives of Biochemistry and Biophysics* **432(1)**:50–57.

444 **Maciejczyk M, Mikoluc B, Pietrucha B, Heropolitanska-Pliszka E, Pac M, Motkowski R,**
445 **Car H. 2017.** Oxidative stress, mitochondrial abnormalities and antioxidant defense in Ataxia-
446 telangiectasia, Bloom syndrome and Nijmegen breakage syndrome. *Redox Biology* **11**:375–383.

447 **Matsushima S, Kuroda J, Ago T, Zhai P, Ikeda Y, Oka S, Fong GH, Tian R, Sadoshima J.**
448 **2013.** Broad suppression of NADPH oxidase activity exacerbates ischemia/reperfusion injury
449 through inadvertent downregulation of HIF-1α and upregulation of PPAR-α. *Circulation*
450 *Research* **112(8)**:1135–1149.

451 **Mehdizadeh R, Parizadeh MR, Khooei, AR, Mehri S, Hosseinzadeh H. 2013.**
452 Cardioprotective effect of saffron extract and safranal in isoproterenol-induced myocardial
453 infarction in wistar rats. *Iranian Journal of Basic Medical Sciences* **16(1)**:56–63.

454 **Moghadam-Kia S, Oddis CV, Aggarwal R. 2016.** Approach to asymptotic creatine kinase
455 elevation. *Cleveland Clinic Journal of Medicine* **83(1)**:37–42.

456 **Moon YJ, Wang X, Morris ME. 2006.** Dietary flavonoids: Effects on xenobiotic and
457 carcinogen metabolism. *Toxicology in Vitro* **20(2)**:187–210.

458 **Naito H, Furukawa Y, Chino D, Yamada C, Hashimoto K. 2000.** Effects of zatebradine and
459 propranolol on canine ischemia and reperfusion-induced arrhythmias. *European Journal of*
460 *Pharmacology* **388(2)**:171–176.

461 **Pangonyte D, Stalioraityte E, Ziuraitiene R, Kazlauskaite D, Palubinskiene J, Balnyte I.**
462 **2008.** Cardiomyocyte remodeling in ischemic heart disease. *Medicina (Kaunas)* **44(11)**:848–854.

463 **Pizzimenti S, Ciamporcero E, Daga M, Pettazzoni P, Arcaro A, Cetrangolo G, Minelli R,**
464 **Powers SK, Murlasits Z, Wu M, Kavazis AN. 2007.** Ischemia-reperfusion-induced
465 cardiacinjury: a brief review. *Medicine and Science in Sports and Exercise* **39(9)**:1529–1536.

466 **Raj Narayana K, Sripal Reddy M, Chaluvadi MR, Krishna DR. 2001**. Bioflavonoids
467 classification, pharmacological, biochemical effects and therapeutic potential. *Indian Journal of*
468 *Pharmacology* **33**:2–16

469 **Shanmugam K, Ravindran S, Kurian GA, Rajesh M. 2018.** Fisetin confers cardioprotection
470 against myocardial ischemia reperfusion injury by suppressing mitochondrial oxidative stress
471 and mitochondrial dysfunction and inhibiting glycogen synthase kinase 3β activity. *Oxidative*
472 *Medicine and Cellular Longevity*

473 **Sun X, Chen RC, Yang ZH, Sun GB, Wang M, Ma XJ, Yang LJ, Sun XB. 2014.** Taxifolin
474 prevents diabetic cardiomyopathy in vivo and in vitro by inhibition of oxidative stress and cell
475 apoptosis. *Food and Chemical Toxicology* **63**:221–232.

476 **Wang YY, Yuan Y, Wang XC, Wang YF, Cheng J, Tian L, Guo XH, Qin DM, Cao WJ.**
477 **2017.** Tilianin post-conditioning attenuates myocardial ischemia/reperfusion injury via
478 mitochondrial protection and inhibition of apoptosis. *Medical Science Monitor* **18(23)**:4490-4499.

479 **Whelan RS, Kaplinskiy V, Kitsis RN. 2010.** Cell death in the pathogenesis of heart disease:
480 mechanisms and significance. *Annual Review of Physiology* **72**:19–44.

481 **Xie X, Feng J, Kang Z, Zhang S, Zhang L, Zhang Y, Li X, Tang Y. 2017.** Taxifolin protects
482 RPE cells against oxidative stress-induced apoptosis. *Molecular Vision* **23**:520–528.
483 **Xuan FF, Jian J. 2016.** Epigallocatechin gallate exerts protective effects against myocardial
484 ischemia/reperfusion injury through the PI3K/Akt pathway-mediated inhibition of apoptosis and
485 the restoration of the autophagic flux. *International Journal of Molecular Medicine* **38(1)**:328-
486 336.
487 **Zhao H, Sapolsky RM, Steinberg G. 2006.** Interrupting reperfusion as a stroke therapy:
488 ischemic postconditioning reduces infarct size after focal ischemia in rats. *Journal of Cerebral*
489 *Blood Flow and Metabolism* **26(9)**:1114-1121.

Figure 1

Figure 1 Experimental protocol

Figure 1. Schematic diagram of experimental protocol. Normal control group (Control); Myocardial I/R control group (I/R); I/R + TAX treatment group (TAX 5 μM); I/R + TAX treatment group (TAX 15 μM).
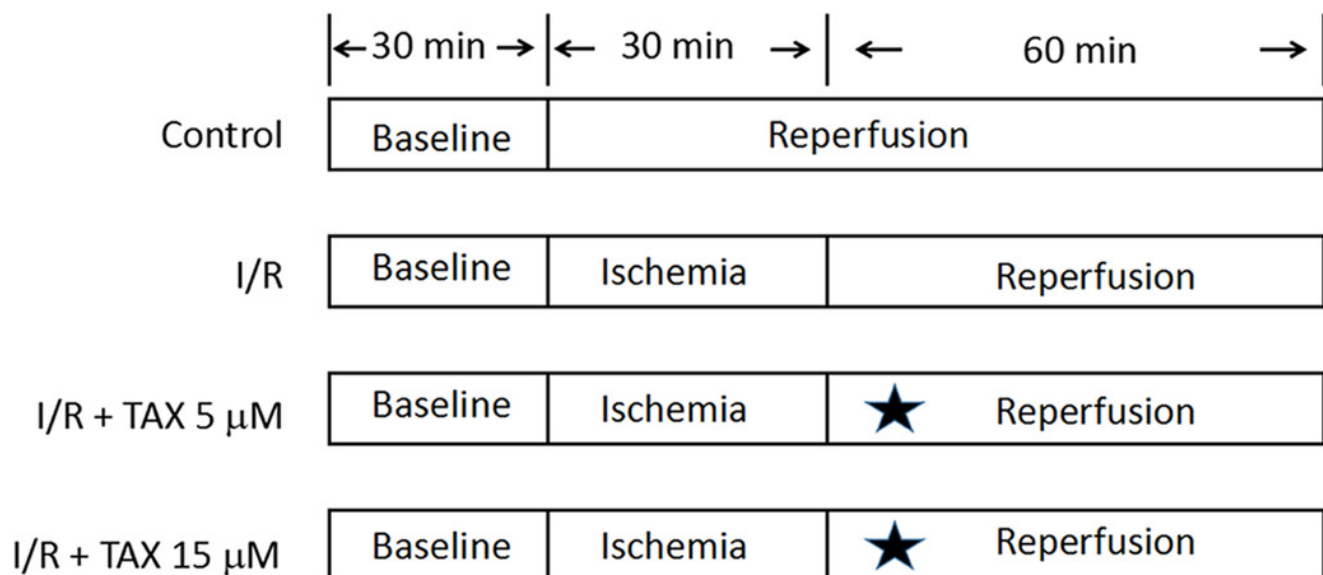
Figure 2

Figure 2. TAX treatment improved the cardiac function recovery of rats during myocardial I/R injury in vitro model.

(A) Heart rate (HR, beat/per min); (B) left ventricular developed pressure (LVDP, mmHg); (C) maximum rate of left ventricular pressure (+dp/dt$_{max,}$ mmHg/s); (D) minimum rate of increase of left ventricular pressure (-dp/dt$_{min}$, mmHg/s); (E) Rate pressure product (RPP, mmHg × bpm); (F) representative left ventricular pressure records in experimental protocol form different experiment groups.
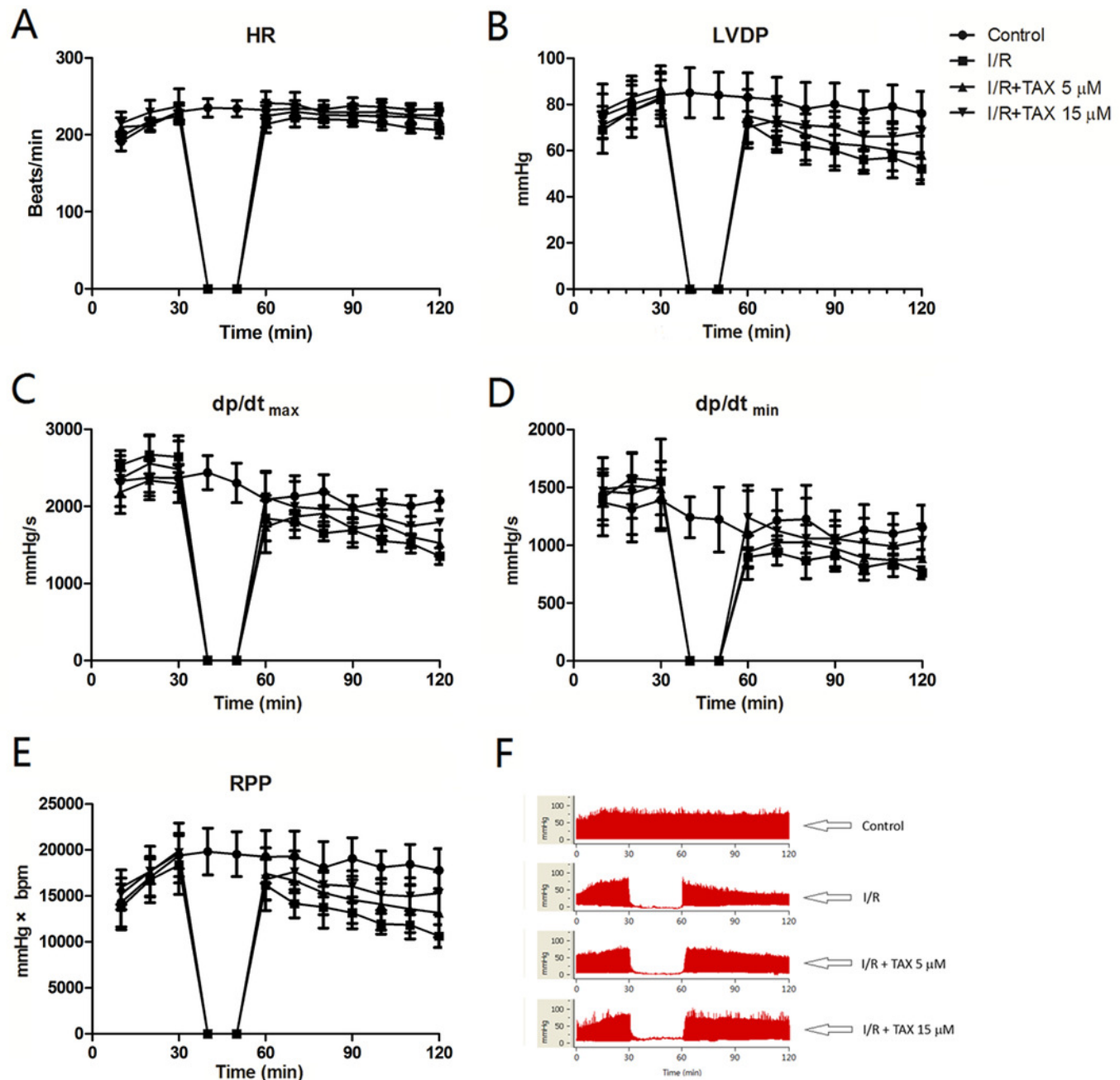
Figure 3

Figure 3. Effect of TAX on injury of cardiomyocytes by measurement of LDH and CK-MB.

The levels of perfusate LDH and CK at different time points in the control, I/R and TAX-treat group (5 μM and 15 μM) are shown. # P < 0.05 and ## P < 0.01 compared with the control group; * P < 0.05 and ** P < 0.01 compared with the I/R group; U/L: international enzyme activity unit per liter.
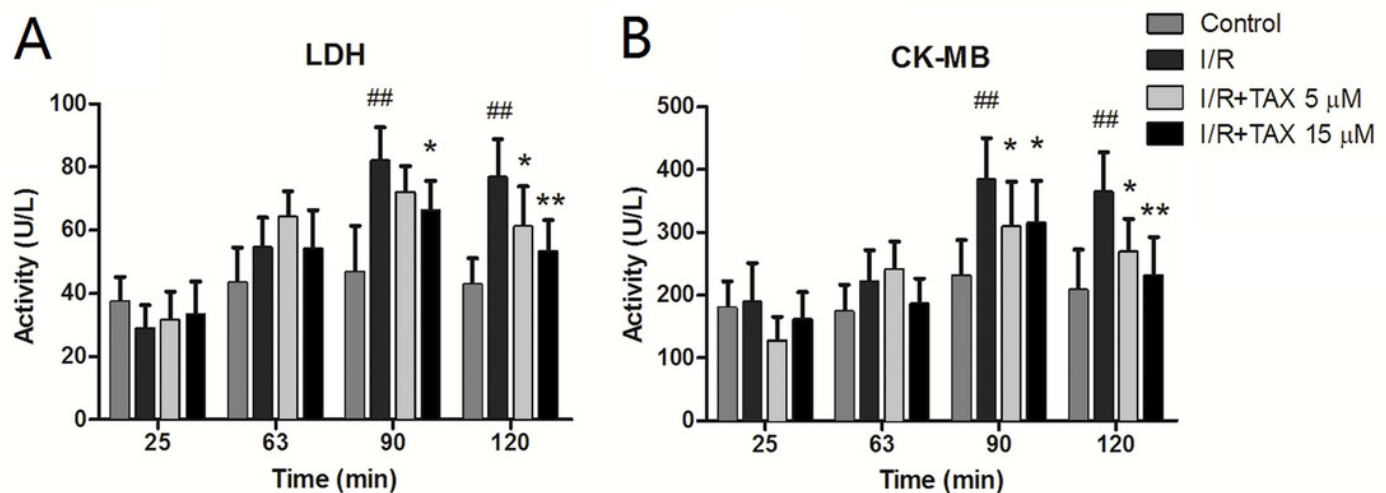
Figure 4

Figure 4. Representative micrographs of HE staining results in various experimental groups.

(A) control group; (B) I/R group; (C) TAX 5 µM group; (D) TAX 15 µM group, n=3 per group, (magnification, ×400), (→) tissue damage and edema.
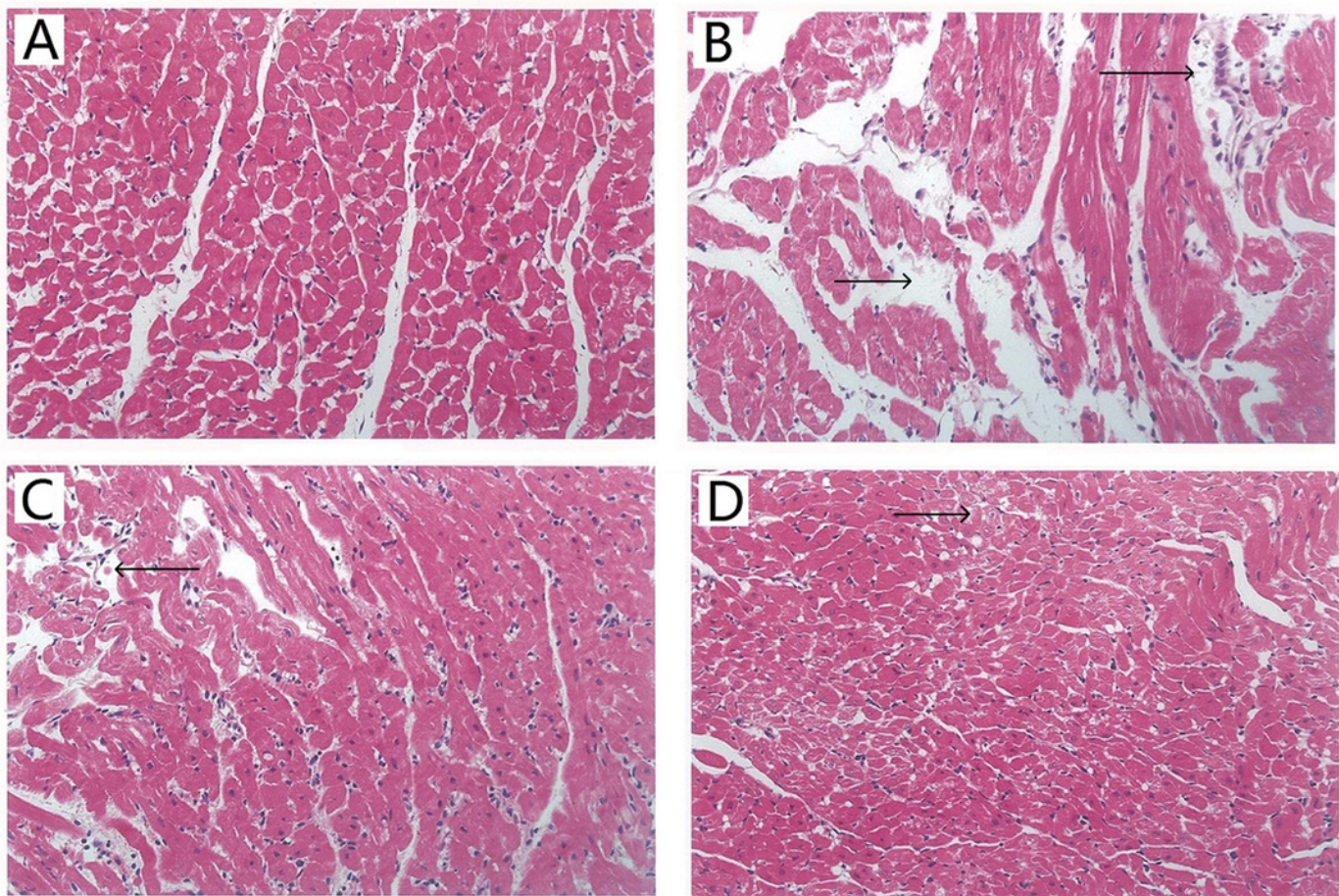
Figure 5

Figure. 5. Effect of TAX on cardiac the activity of SOD and GSH-PX, contents of MDA.

Values are presented as mean ± SD. # P < 0.05 and ## P < 0.01 compared with the control group; * P < 0.05 and ** P < 0.01 compared with the I/R group. U/mgprot: international enzyme activity unit per milligram tissue protein.
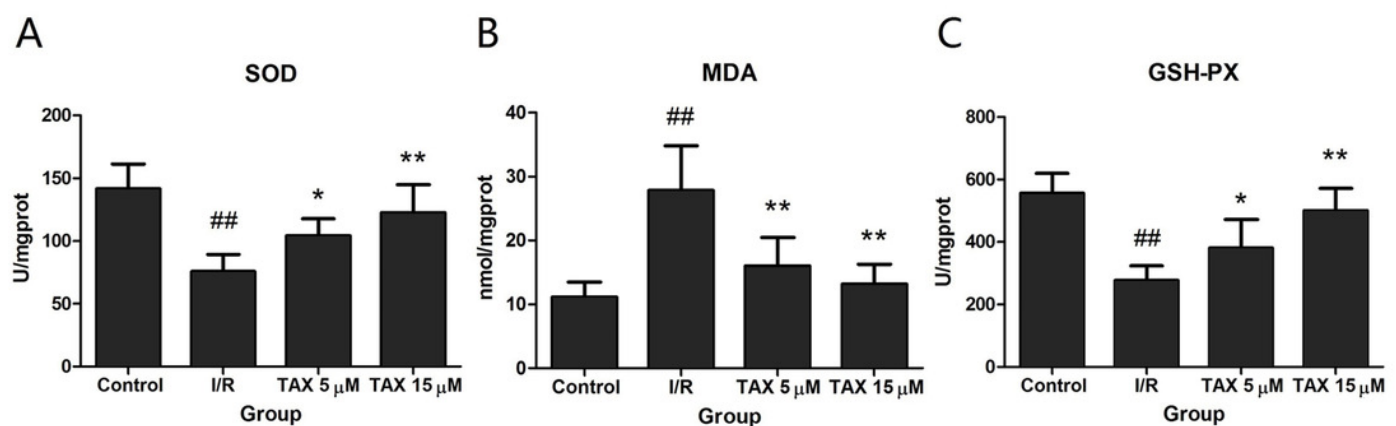
Figure 6

Figure 6. Effect of TAX on the expression of Cyt-c, Bax and Bcl-2 protein.

# P < 0.05, ## P < 0.01 vs. Control group; * P < 0.05, ** P < 0.01 vs. IR group. ng/mgprot indicate the nanogram level of the target protein per milligram total protein.
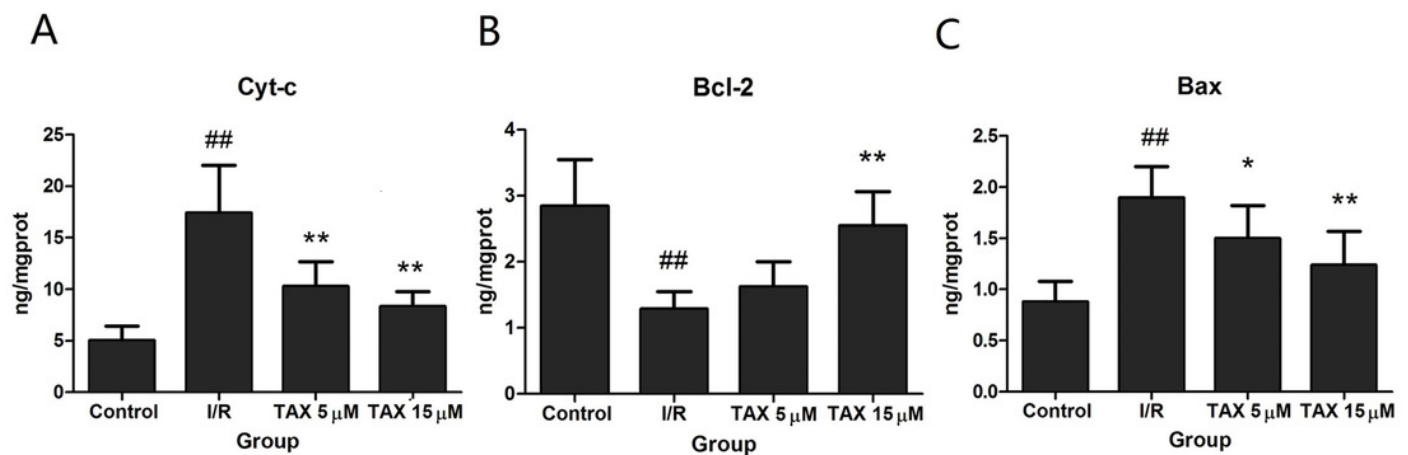
Figure 7

Fig. 7. The changes in the levels of caspase 3, and caspase 9 at the end of reperfusion.
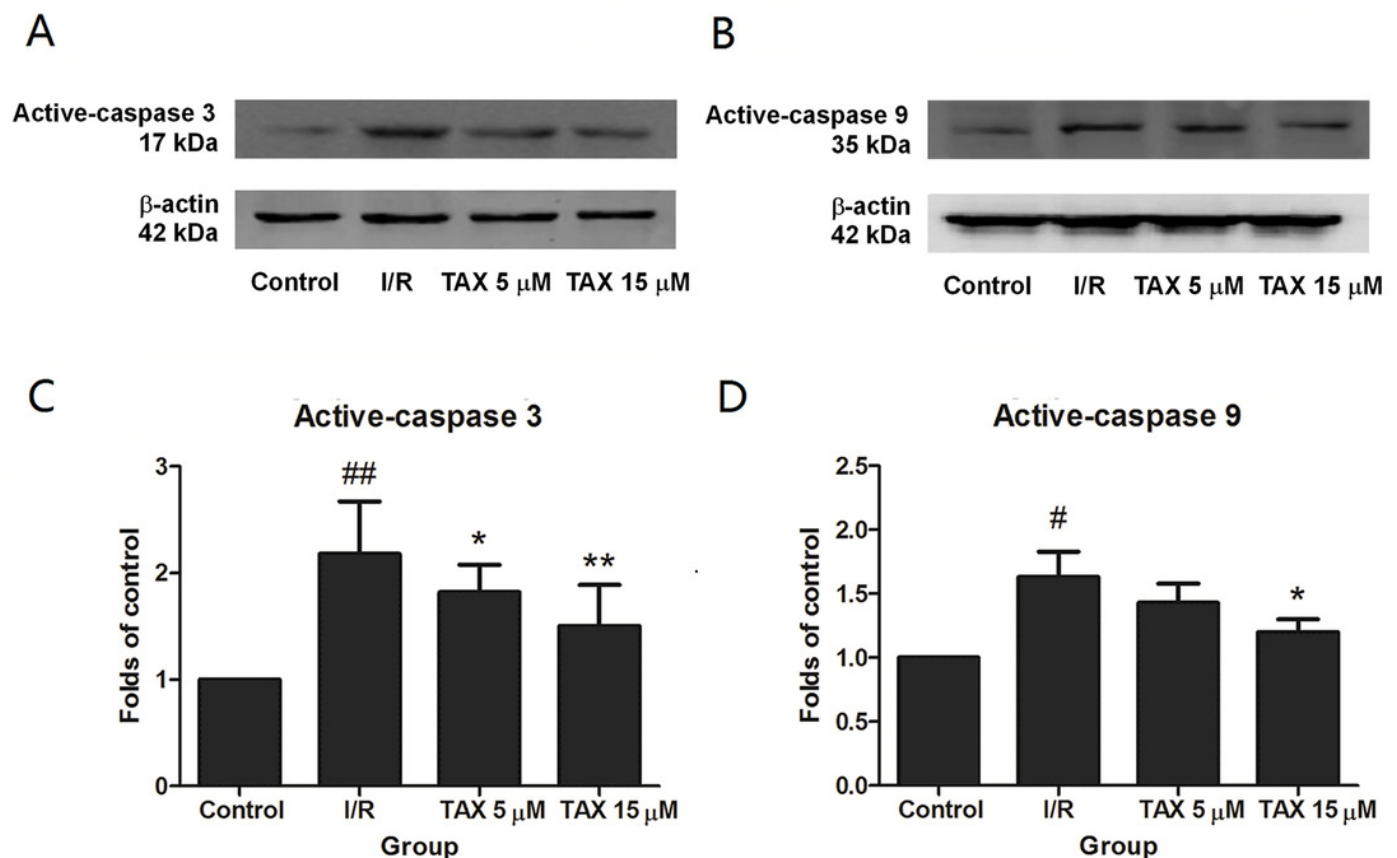
Figure 8

Figrue 8. Effect of taxifolin on cardiomyocytes apoptosis in different experimental groups.

(A) control group; (B) I/R group; (C) I/R + TAX 5 μM group; (D) I/R + TAX 15 μM group. n=3 per group, 20X, Scale bar 50 μm, (→) positive stain